Wintertime East Asian Jet Stream and Its Association With the Asian–Pacific–American Climate

Song Yang[1], K.–M. Lau, and K.–M. Kim[2]

NASA/Goddard Space Flight Center
Laboratory for Atmospheres
Climate and Radiation Branch
Greenbelt, Maryland 20771, USA

1. Introduction

The wintertime upper–tropospheric westerly jet stream over subtropical East Asia and western Pacific, often referred to as East Asian Jet (EAJ), is an important atmospheric circulation system in the Asian–Pacific–American (APA) region. It is characterized by variabilities on a wide range of time scales and exerts a strong impact on the weather and climate of the region. On the synoptic scale, the jet is closely linked to many phenomena such as cyclogenesis, frontogenesis, blocking, storm track activity, and the development of other atmospheric disturbances. On the seasonal time scale, the variation of the EAJ determines many characteristics of the seasonal transition of the atmospheric circulation over Asia. The variabilities of the jet on these time scales have been relatively well documented (e.g., Yeh et al. 1959, Palmén and Newton 1969; Zeng 1979).

It has also been understood that the interannual variability of the EAJ is associated with many climate signals in the APA region. These signals include the persistent anomalies of the East Asian winter monsoon and the changes in diabatic heating and in the Hadley circulation (Bjerknes 1966; Chang and Lau 1980; Huang and Gambo 1982; Kang and Held 1986; Tao and Chen 1987; Lau et al. 1988; Yang and Webster 1990; Ding 1992; Webster and Yang 1992; Dong et al. 1999). However, many questions remain for the year–to–year variabilities of the jet and their relation to the APA climate. For example, what is the relationship between the EAJ and El Nino/Southern Oscillation (ENSO)? Will the jet and ENSO play different roles in modulating the APA climate? How is the jet linked to North Pacific sea surface temperature (SST) and the Pacific/North American (PNA) teleconnection pattern?

In this study, we address several issues related to the wintertime EAJ with a focus on interannual time scales. We will examine the association between the jet core and ENSO, which has always been overshadowed by the relationship between ENSO and the upper–tropospheric winds over northern extratropics of the central Pacific. We will investigate the linkage of the jet to variabilities of the Asian winter monsoon, tropical convection, and upper tropospheric wave patterns. We will also explore the relationship between the jet core and extratropical SST with an aim at providing helpful information for improving our understanding of the connection of the EAJ to surface boundary conditions. The analysis is expected to provide information that is helpful for improving regional climate predictions.

2. Data sets

The primary data set used in this study is the reanalysis product from the US NOAA National Centers for Environmental Prediction and National Center for Atmospheric Research. Other data include the surface air temperature from US NASA Goddard Institute for Space Studies, precipitation from Global Precipitation Climatology Project, and the snow cover data from NOAA. Southern Oscillation index (SOI) and the NOAA reconstructed SST are also analyzed. These data sets cover different time periods and are distributed in different spatial resolutions. In this study, seasonal averages, computed from monthly mean data, are analyzed with an emphasis on the December–January–February (DJF) averaged values.

1   SAIC/General Sciences Corporation, Beltsville, MD, USA
2   Universities Space Research Association, NASA/Goddard Space Flight center, Greenbelt, MD, USA.

Corresponding author address: Dr. Song Yang, NASA/Goddard Space Flight Center, Climate and Radiation Branch, Mail Code 913, Greenbelt, MD 20771, USA.

3. Results

3.1 ENSO and EAJ related circulation patterns

During the northern winter, the largest values of global 200 mb zonal wind (U200) exist over East Asia, with a center larger than 70 m/s over the ocean south of Japan. However, the maximum variances of U200 do not occur within the maximum centers of the wind but emerge from the tropics and subtropics of the central−eastern Pacific and the North Atlantic east of Canada. The variability of U200 is actually small over entire Asia. Figure 1a that the variations of the U200 maxima over East Asia are not strongly related to ENSO. The correlation between SOI and the wind near the EAJ core is close to zero. The winds over subtropical Asia and Pacific west of the dateline have little link to the Southern Oscillation.

Out of 50 DJFs during 1949−1999, the jet maximum appears over 32.5N, 140E in 15 DJFs. Its maximum is mostly located over 32.5N and shifts occasionally northward to 35N. Longitudinally, this maximum shifts westward or eastward by about 10 degrees. The small migration of the jet core, especially latitudinally, facilitates the construction of an index that measures the variability of the EAJ. We define this index as the yearly DJF U200 averaged within 30−35N and 125−165E. The correlation between this EAJ index and the global grid−point U200 is presented in Fig. 1b. The dominant feature of the figure is that the intensification of the jet is accompanied by a reduction of westerly component over the northern extratropics from southeastern Russia to the Bering Sea and over the tropical Pacific. (The tropical easterlies also intensify, though not significantly, when the EAJ is strong.) The strengthening EAJ core increases the U200 upstream and downstream, although the downstream intensification is more obvious. Importantly, the pattern of Fig. 1b differs substantially from the ENSO−related pattern shown in Fig. 1a. Besides the signal over the tropical monsoon region of Asia−Australia, the ENSO−related features over the Pacific are mainly limited to the east of the dateline. On the contrary, the signals that are related to the EAJ appear mainly over East Asia and the western−central Pacific. At the locations where jet−U200 correlation is strongest, the SOI−U200 correlation is among the weakest. Thus, the teleconnection pattern linked to the EAJ is clearly distinct from that associated with ENSO, indicating that the EAJ and ENSO link to two different modes of the atmospheric circulation in the APA region.

The above−discussed features are confirmed by the empirical orthogonal function (EOF) analysis for U200 (figures not shown). The first EOF mode captures the ENSO−related features that indicate increase in the subtropical central Pacific U200 during El Nino winters and decrease in the wind during La Nina winters. The second mode exhibits northwest−southeast oriented signals extending from extratropical Asia to tropical central Pacific, similar to those shown in Fig. 1b.

Figure 2 shows the pattern of regressions of 850 mb wind vectors against the first and second principal components from the EOF analysis of U200. (The shadings indicate the areas over which the correlation between the principal component and the wind component, zonal or/and meridional, is significant at or above the 99% confidence level.) There exist several differences between the two panels of Fig. 2. In spite of the similarity over the extratropical Pacific north of 25N and east of 150E, the changes associated with the increase in the westerlies over subtropical central Pacific (Fig. 2a) are nearly in an opposite sign with those linked to the EAJ intensification (Fig. 2b). Figure 2a shows a decrease in the trade winds over the tropical central Pacific and in the westerlies over the tropical Indian ocean, which causes a "divergence" over Indonesia and the tropical western Pacific. However, the trade winds and the westerlies become stronger when the EAJ is strong. An area of "convergence" appears over Southeast Asia including the South China Sea, consistent with the increase in local convection and precipitation (figures not shown). During El Nino, the Asian winter monsoon becomes slightly weaker, together with a clockwise pattern over southern Asia and the nearby oceans (Fig. 2a). However, when the EAJ is strong, the East Asian winter monsoon intensifies. In particular, the northerly component over East Asia and the western Pacific strengthens from the mid−latitudes to the tropics (Fig. 2b). The figure also shows that the change in the monsoon is part of the broad−scale counterclockwise pattern over the North Pacific. A remarkable feature of Fig. 2 is that while the first principal component links to dominant signals over the central−eastern Pacific, the second principal component links strongly to the signals over the western Pacific.

3.2 EAJ's climate impact

It has been presented in Fig. 2 that, compared with ENSO, the EAJ connects more strongly to the

East Asian winter monsoon. For the period from 1950–99, the correlation between the jet and the 850 mb meridional wind averaged over 20–40N, 100–140E is –0.51. However, the correlation between SOI and the monsoon is only –0.37.

Here, we demonstrate more features about the impact of the EAJ on the APA climate. Figure 3 shows the changes, between the strong and weak jets, in 500 mb geopotential height (H500), stationary wave activity flux (SWAF), and snow over. The year–to–year variability of the intensity of the jet core is associated with significant change in the atmospheric wave pattern in the APA region. Two important features associated with strong EAJ can be found in Fig. 3a. Firstly, the East Asian Trough deepens and H500 decreases to its east but increases to its west. Thus, the change in the EAJ is accompanied by an adjustment of the large–scale circulation system over Asia and the Pacific. This adjustment increases the north–south pressure gradient in the Asian–Pacific region and favors a southeastward intrusion of the cold air from Siberia, intensifying the East Asian winter monsoon. Secondly, associated with the strong jet is a stronger PNA pattern, which links closely to the climate of eastern Pacific and North America.

Figure 3b shows the change in SWAF (Plumb 1985) between the strong and weak jets. Following Yang and Gutowski (1994), we reveal the features of the horizontal components at 300 mb (vectors) and the vertical component at 850 mb (contours and shadings). In both strong and weak EAJ cases, the wave activities propagate mainly eastward and upward. They emanate from eastern Asia, eastern Pacific, and western Atlantic. Obviously, the wave activities propagate southward from these three locations. When the EAJ weakens, the wave activities diminish in almost entire northern extratropics. Major reduction occurs in the eastward propagation over East Asia, the southeastward propagation over eastern Pacific and the Atlantic, and the northeastward propagation over North America. Also reduced remarkably is the upward propagation over East Asia and the eastern Pacific. When the EAJ is weak, the northeastward propagation of the SWAF over East Asia north of 40N weakens as well. This weakening is consistently accompanied by an intensification of the upward propagation over the Sea of Okhotsk and nearby regions. Figure 3b suggests a teleconnection between EAJ and the atmospheric circulation over the eastern Pacific, North America, and even the Atlantic Ocean.

Figure 3c provides information about the EAJ–related changes in snow area and frequency. The value shown for each grid is the difference, between the strong and weak jets, in the number of months when snow is present. Data from the November–April of six years of strong jet and six years of weak jet are used in the calculation. For example, the number "5" at a specific grid means that snow exists in that grid more frequently in the strong jet group than in the weak jet group by five months. The figure indicates that, when the EAJ is strong, snow appears more frequently and extensively over Asia, mainly between 37N and 55N. Figure 3c also indicates that strong EAJs link to less (more) frequent snow over the western (eastern) United States.

3.3 Linkage of EAJ to North Pacific SST

Because of the relationship between the EAJ and PNA pattern (Fig. 3a), we assume that the variability of the jet is associated with the changes of the North Pacific SST (NPSST), which are not necessarily related to those of ENSO. Figure 4 depicts the second mode of the singular value decomposition (SVD) analysis of the NPSST and northern hemisphere U200. (The first mode, which is substantially different from the second mode, mainly captures the ENSO type SST–U200 relation and is not discussed here.) Associated with the cooling in the tropics–subtropics and warming in the extratropics are the weakening of EAJ and the changes in the North Pacific U200 that are similar to the pattern shown in Fig. 1b. Thus, a stronger EAJ is accompanied by colder SST underneath. It should also be pointed out that the SVD pattern experiences very small change when the entire Northern Hemisphere SST is applied in the calculation. This suggests a weak tie of the EJA with the SSTs of the North Atlantic and northern Indian Ocean.

Although the result presented in Fig. 4 does not suggest a cause–and–effect relationship between the EAJ and NPSST, it shows an important feature. The EAJ core has weak association with ENSO (and thus Nino–3 SST) but links closely to the NPSST. This feature also implies that the EAJ and ENSO link differently to the NPSST. Figure 4c indicates that the variation of the EAJ–NPSST association occurs on time scales different from those of ENSO. It is characterized by relatively longer time scales. The interdecadal variability of this association and its role in the variations of APA climate systems (e.g., the

Asian winter monsoon and PNA pattern) and the climate in APA region is currently under investigation.

4. Summary

In this study, we have demonstrated the importance of the wintertime EAJ for the variations of the APA climate. We have emphasized the variability of the jet core and its association with the East Asian winter monsoon, tropical convection, upper tropospheric wave patterns, and the teleconnection patterns outside the extratropical Asian–Pacific region.

The EAJ and ENSO link to two very different modes of atmospheric circulation over the APA region. While ENSO causes robust, PNA–like signals to the east of the dateline, the EAJ links to a teleconnection pattern whose major climate anomalies appear over the Asian continent and western Pacific (west of the dateline). A strong jet is accompanied clearly by a strong Asian winter monsoon that leads to cold climate over Asia and the Pacific and intensifying convection over the tropics. Changes in the jet are associated with broad–scale modification in the upper tropospheric wave patterns that lead to downstream climate anomalies over the eastern Pacific. Through this downstream influence, the EAJ causes climate signals in North America as well. Associated with a strong EAJ are the warming and less snow cover in the western but reverse anomalies in the eastern United States, although these signals are relatively weaker than the jet–related anomalies in East Asia. In addition, the EAJ is closely associated with a NPSST pattern that has little link to ENSO, indicating the EAJ and ENSO are associated with NPSST in very different ways.

5. References

Bjerknes, J., A possible response of the atmospheric Hadley circulation to equatorial anomalies of ocean temperature. *Tellus, 18,* 820–829.

Chang, C.–P., and K.–M. Lau, 1980: Northeasterly cold surges and near–equatorial disturbances over winter MONEX area during December 1974: Part II: Planetary scale aspects. *Mon. Wea. Rev.,* **108,** 298–312.0.

Ding, Y.–H., 1992: Summer monsoon rainfalls in China. *J. Meteor. Soc. Japan,* **70,** 373–396.

Dong, M., J. Yu, and S. Gao, 1999: A study on the variations of the westerly jet over East Asia and its relation with the tropical convective heating. *Chinese J. Atmos. Sci.,* **23(1),** 62–70.

Huang, R., and K. Gambo, 1982: The response of a hemispheric multilevel model atmosphere to forcing by topography and stationary heat sources. *J. Meteor. Soc. Japan,* **60,** 78–108.

Kang, I.–S., and I.–M. Held, 1986: Linear and nonlinear diagnostic models of stationary eddies in the upper troposphere during northern summer. *J. Atmos. Sci.,* **43,** 3045–3057.

Lau, K.–M., G.–J. Yang, and S.–H. Shen, 1988: Seasonal and intraseasonal climatology of summer monsoon rainfall over East Asia. *Mon. Wea. Rev.,* **116,** 18–37.

Palmén, E., and C. W. Newton, 1969: Atmospheric Circulation Systems: Their Structure and Physical Interpretation. Academic Press, Inc., San Diego, California, pp. 603.

Plumb, R. A., 1985: On the three–dimensional propagation of stationary waves. *J. Atmos. Sci.,* **42,** 217–229.

Tao, S.–Y., and L.–X. Chen, 1987: A review of recent research of the east Asian summer monsoon in China. In *Monsoon Meteorology,* Ed. By C.–P. Chang and T. N. Krishnamurti, Oxford Univ. Press, pp. 60–92.

Webster, P. J., and S. Yang, 1992: Monsoon and ENSO: Selectively interactive systems. *Quart. J. Roy. Meteor. Soc.,* **118,** 877–926.

Yang, S., and W. J. Gutowski, 1994: GCM simulations of the three–dimensional propagation of stationary waves. *J. Climate,* **7,** 414–433.

Yang, S., and P. J. Webster, 1990: The effect of summer tropical heating on the location and intensity of the extratropical westerly jet streams. *J. Geophys. Res.,* **95,** 18705–18721.

Yeh, T.–C., S.–Y. Dao, and M.–T. Li, 1959: The abrupt change of circulation over the Northern Hemisphere during June and October. In *The Atmosphere and the Sea in Motion,* Ed. By B. Bolin, Rockefeller Inst. Press, New York, pp. 249–267.

Zeng, Q. C., 1979: Mathematical and Physical Basis for Numerical Weather Forecast. Science Press, Beijing, China, pp. 314.
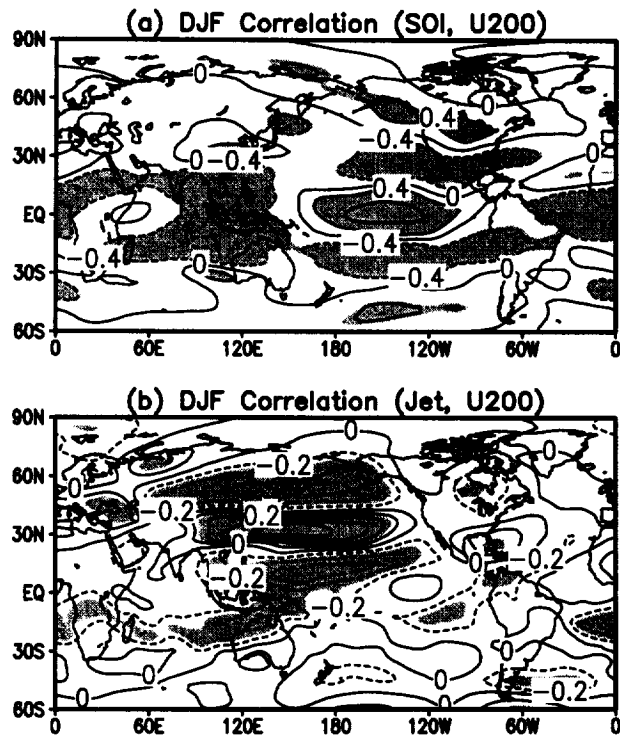
Fig. 1. (a) DJF correlation between SOI and NCEP/NCAR reanalysis U200 for 1949–99. (b) DJF correlation between the EAJ and U200. Contour intervals: 0.4 in (a) and 0.2 in (b).
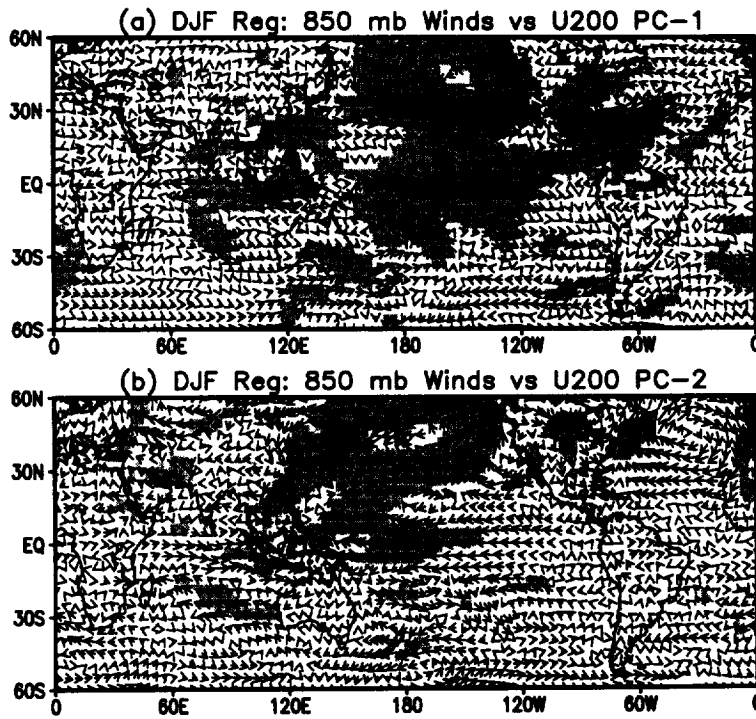

Fig. 2. (a) DJF regressions (in m/s) of 850 mb winds against the first principal component from the U200 EOF analysis. (b) Same as (a), but for the second principal component.

(a) U200   MODE 2 (14.0%)

(b) SST

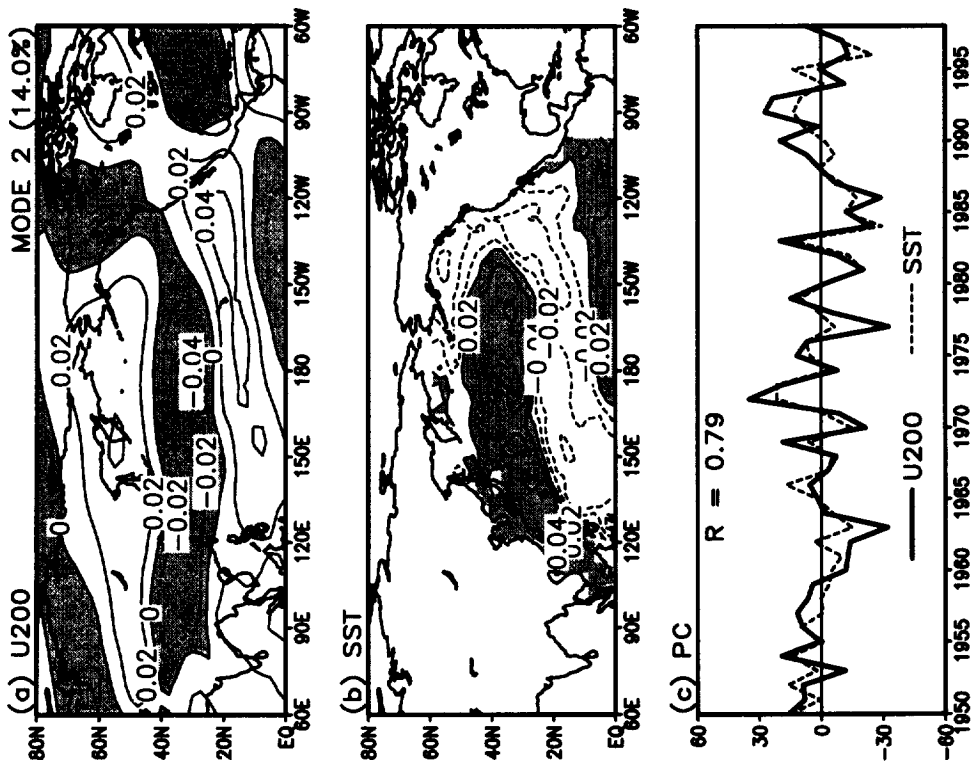(c) PC   R = 0.79

———— U200
- - - - SST

Fig. 4. The second mode of SVD of the norther hemisphere
U200 (a) and North Pacific SST (b) for DJF, together with
the corresponding time series (c).

(a) Nov–Apr Snow Month Diff (S–W)

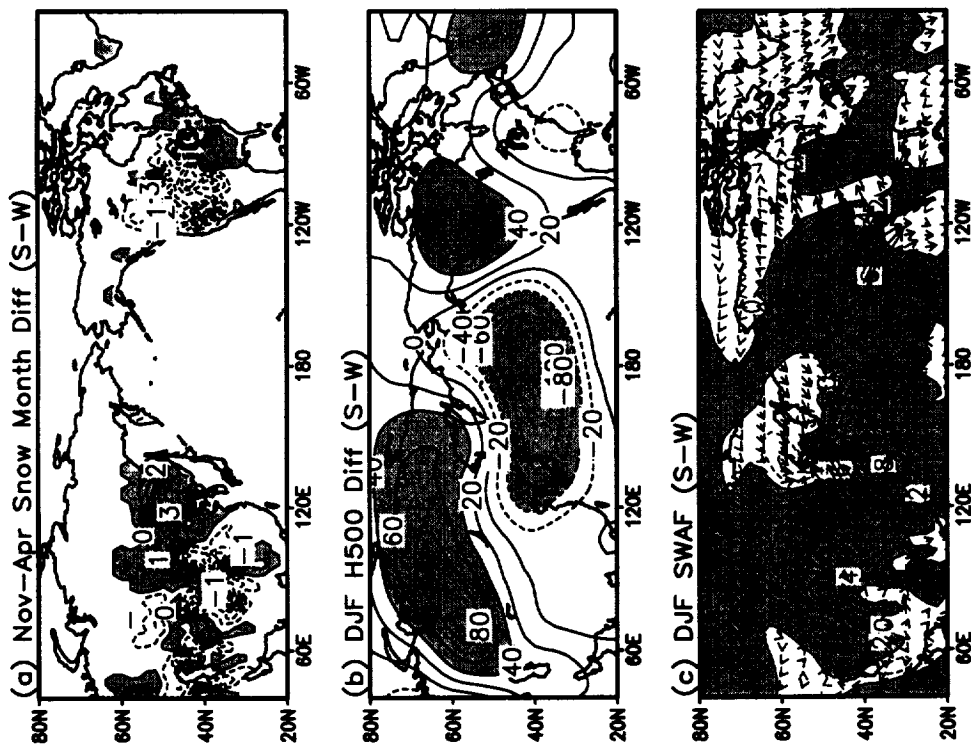(b) DJF H500 Diff (S–W)

(c) DJF SWAF (S–W)

Fig. 3. Differences, between strong and weak EAJs, in the
number of snow cover (a; in month), H500 (b; in m), and
SWAF (c). In (c), the vectors are for 300 mb horizontal
component (m²s⁻²) and the contours and shades for 850
mb vertical component (x10⁴ m²s⁻²).